*Acta Geologica Polonica*, Vol. 73 (2023), No. 1, pp. 103–114
DOI: 10.24425/agp.2022.143595

# Provenance of quartz debris in the Central Western Carpathians at the end of the Triassic, as indicated by cathodoluminescence colours

MAREK VĎAČNÝ* and JOZEF MICHALÍK

*Earth Science Institute of the Slovak Academy of Sciences, Dúbravská cesta 9, P.O. BOX 106, 840 05 Bratislava, Slovakia; e-mails: marek.vdacny@savba.sk; jozef.michalik@savba.sk*
**Corresponding author*

ABSTRACT:

Vďačný, M. and Michalík, J. 2023. Provenance of quartz debris in the Central Western Carpathians at the end of the Triassic, as indicated by cathodoluminescence colours. *Acta Geologica Polonica*, **73** (1), 103–114. Warszawa.

Lithic fragments including quartz grains occur infrequently in the shallow-marine limestone sequence of the Fatra Formation deposited in the tensional intra-shelf depression of the Central Western Carpathians during the Rhaetian. Nevertheless, their study can bring data answering questions of sources, palaeogeodynamic arrangement, and processes at the end of the Triassic. In this study, we examined optically the cathodoluminescence (CL) colours of single quartz grains from the Kardolína section (Tatra Mts, Slovakia). These colours reveal a dominance of grains derived from regionally metamorphosed and plutonic rocks. Grains of hydrothermal and pegmatite origin are less frequent. Some of the quartz grains show recycled cement rims suggesting at least a second cycle origin. This sedimentary basin was situated near to the passive margin formed by the Variscan consolidated terrains of the Vindelician Highlands. Our study of the CL colours of quartz grains contributes to the elucidation of the nature of the rocks of the vanished Vindelician mountain belt.

**Key words:** Aeolian quartz grains; Cathodoluminescence; Provenance; Fatra Formation; Zliechov Basin; Uppermost Triassic; Slovakia.

## INTRODUCTION

The end of Triassic time saw the major transition from an arid type of climate to a humid monsoonal regime (Michalík *et al.* 2010). Rapid breakup of the vast Pangaea supercontinent was accompanied by accelerated weathering of newly elevated areas, by intensification of river transport, and by deposition of weathered rock products in basinal systems.

During these times, the Carpathian part of the northern Tethyan shelf was also influenced by input of terrestrial debris from the hinterland. In emerged areas, terrestrial Carpathian Keuper deposits were covered by the Rhaetian Tomanová Formation composed of lacustrine to palustrine black silty shales rich in kaolinite and plant fragments, intercalations of quartz sandstones with dinosaur footprints, and sphaerolitic iron ores (Michalík *et al.* 1976, 1988; Niedźwiedzki 2005, 2011; Lintnerová *et al.* 2013). The overlying Lower Jurassic Dudziniec Formation consists of shallow-marine sandy limestones.

The Zliechov Basin, located further to the south, was submerged by a shallow sea basin with sedimentation of the bioclastic limestones of the Fatra Formation. The benthic fauna comprises Rhaetian index foraminifers (*Triasina hantkeni*), bivalves (*Rhaetavicula contorta*), corals (*Retiophyllia paraclathrata*), brachiopods (*Austrirhynchia cornigera*), and other


Text-fig. 1. Simplified map showing the location of the studied Kardolína section in the Tatra Mountains (modified from Michalík *et al.* 2010).

organic remnants (Gaździcki *et al.* 1979; Michalík *et al.* 2007, 2013; Čerňanský *et al.* 2020). The Fatra Formation was covered by the Hettangian marine shales of the Kopieniec Formation.

Sedimentological study indicates a relatively low content of small quartz grains (2–4%) in the Fatra Formation limestones pointing to low intensity of river transport in a dry climate. More abundant quartz grains occur in outcrops in the Tatra Mts (from 3 to 16%, in some beds up to 39%), and these suggest the palaeogeographic proximity of this area to periodical fluvial clastic transport routes (Michalík *et al.* 2013). Irregular distribution of very fine-grained quartz derived from distant extrabasinal sources evokes the question of the origin and input of this quartz dust, and of the palaeogeodynamic model of the adjacent land.

However, conventional petrographic analysis could hardly help in this respect. We therefore turned to the more sophisticated cathodoluminescence (CL) microscopy. Indeed, CL reveals many features which are invisible with the petrographic microscope (e.g. Sippel 1968; Matter and Ramseyer 1985). Grains of quartz of diverse origin can be characterised on the basis of their CL colour and used in provenance studies (e.g. Zinkernagel 1978; Marshall 1988; Götze 1996; Boggs 2009). Thereby, the CL is a powerful technique and has potential in solving problems of sediment provenance (e.g. Omer 2015; Sales de Oliveira *et al.* 2017; Leila *et al.* 2018).

In the context of the above, the aim of our research is to reconstruct parent rock assemblages of Rhaetian aeolian quartz grains incorporated in the Fatra Formation in the Tatra Mts (Western Carpathians, Slovakia) (Text-fig. 1) using the CL technique. This reconstruction will allow us to test the validity of existing palaeogeographic models and thus to enhance our knowledge of the geodynamic situation of this area at the end of Triassic.

## GEOLOGICAL SETTING

The Rhaetian Fatra Formation (Text-fig. 2) in the small pull-apart Zliechov Basin (forming a part of the present-day Fatric nappe structure of the Central Western Carpathians) has attracted the attention of researchers for decades (e.g. Michalík 1977; Gaździcki 1983; Michalík 1993; Tomašových 2004; Michalík *et al.* 2013; Onoue *et al.* 2022). It was deposited in a marine, shallow-water intra-platform, mainly carbonate setting in the Fatric Unit (Michalík 1982). The Rhaetian age of this formation has been corroborated by the first occurrence of foraminifers (*Glomospirella friedli* and *Triasina hantkeni*; Gaździcki 1983) and brachiopods (*Austrirhynchia cornigera*; Tomašových 2004). The Fatra Formation rests transgressively on terrestrial Carpathian Keuper deposits (e.g. Michalík 1974, 1977) and is overlain with a strict contact by the marine shales of the Hettangian Kopieniec Formation (e.g. Tomašových and Michalík 2000).

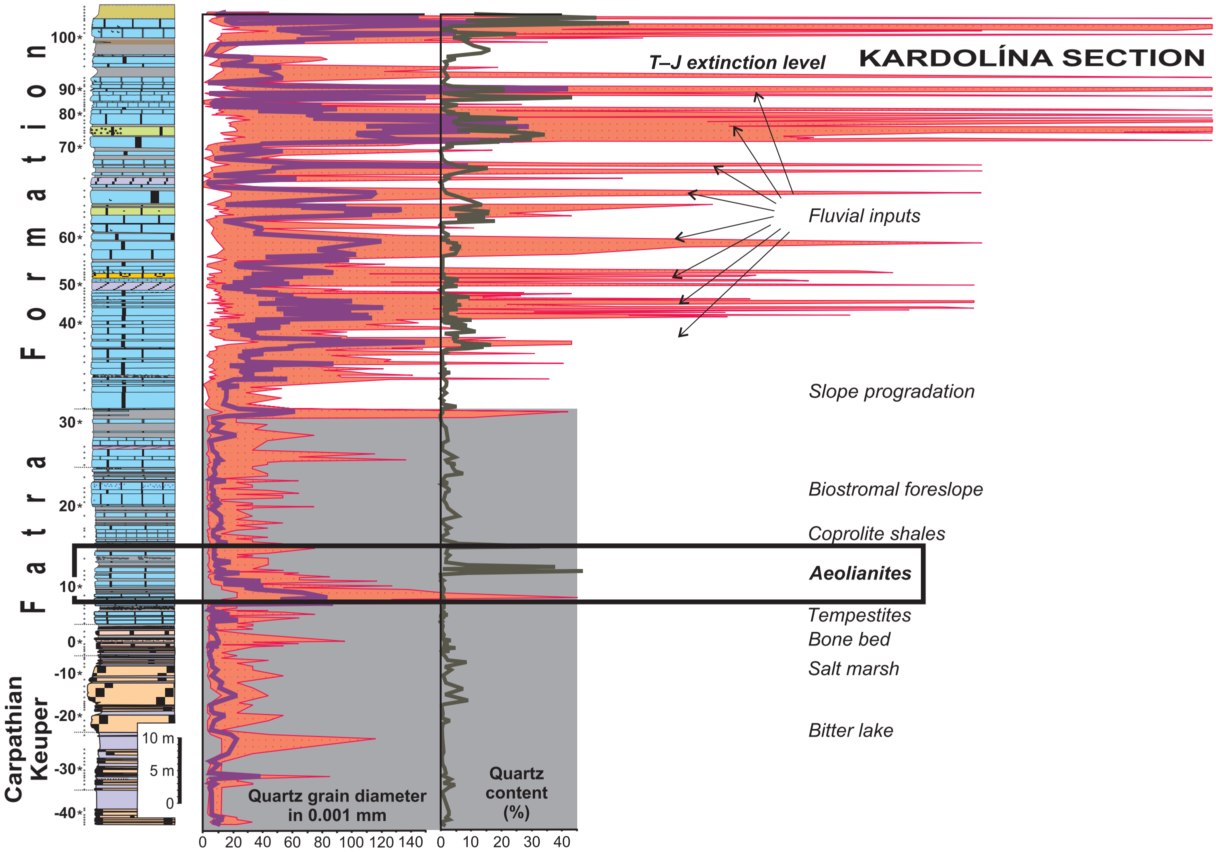


Text-fig. 2. Quartz grain size (average size denoted by thick line) and percentage content of quartz grains of the Kardolína section sequence and interpretation of depositional environment. Data marked with a grey rectangle are from Michalík *et al.* (2013). Other data are new and original. The beds discussed in this study are marked with a black rectangle. Asterisks show numbering of beds.

A 30-m-thick sequence of mixed terrigenous, lacustrine, fluvial, and aeolian variegated, greenish, and violet-red dolomitic claystone with occasional intercalations of pale greenish-grey clayey dolostone, exposed in the Kardolína section in the Belianske Tatry Mts, represents the uppermost part of the Carpathian Keuper sequence (Text-fig. 2). The thickness of the Fatra Formation is variable (from 25 meters to a maximum of 116 meters; Michalík *et al.* 2007). It has been divided into five informal members by Michalík (1977) and Gaździcki *et al.* (1979): the “basal member”, two “biostromatic members”, separated by the “barren interval” of dolomite, dolomitized limestone, and redeposited carbonate, and the “transitional member” at the top of the Fatra Formation sequence containing several uncommon beds (micritic ostracodal limestones with undulating bedding planes, coquinas with bivalves and foraminifers, and ferruginous oolitic limestones).

Recently, eighteen sedimentary cycles attributed to short eccentricity (100 ka) periodicities were distinguished in the Kardolína section (Michalík *et al.* 2007, 2010, 2013). This section represents the most complete outcrop of the Fatra Formation (Text-fig. 2), deposited in a more rapidly subsiding part of the basin. It shows a more complete stratigraphy of the “basal member”, comprising here three different cycles.

1. The lowermost cycle is consisted of thinning- and fining-upward (65 to 20 cm) grey biomicrite containing dispersed quartz grains (0.005 to 0.2 mm in diameter) and numerous ostracod tests. Higher up, the dolomicrosparite content increases (up to 9%) and fragments of plants become abundant. Dolostone layers are followed by 330-cm-thick brown claystone interval. Fine clastic laminae in Beds -4, -3 and in the “zero beds” contain numerous foraminifers (*Agathammina austroalpina*), suggesting sedimentation in low-energy environment, most likely on tidal flats. Clastic quartz particles are rare and rather small, bearing signs of wind, not of river transport. Biodetrital limestone is followed by brown claystone

and this is intercalated by dolostone layers with bone-bed type surfaces.

2. Grey biomicrites to calcarenites containing frequent mollusc and brachiopod shells (occasionally with distorted geopetal fillings). There are erosional marks and load casts on the layer bases, and gradation of fragments occurs frequently, suggesting an origin in distal tempestite lobes laid on a soft marly bottom. During the sedimentation of this cycle, intensive storm activity seems to have been a typical feature of the environment.

3. This fining- and thinning-upward cycle (12 m thick) of dark brown aleuritic marl and argillaceous limestone contains abundant subangular quartz grains (0.02 to 0.03 mm) indicating aeolian transport. Sea storms, which dominate this part of the sequence, were subsequently replaced by terrestrial dust storms bringing fine quartz debris.

Higher up, the major part of the Fatra Formation sequence bears signs (mollusc shells, crinoid ossicles, foraminifers, and other fully-marine fauna) of a stabilised marine regime. The terrigenous quartz grain fraction and the ferruginous content increase upwards. They record the 100 ka periodicity of monsoon-like maxima of terrigenous flux (Michalík *et al.* 2007, 2010). The contact with overlying non-carbonate shaly Kopieniec Formation is sharp.

In this study, we concentrated on the nature of the peculiar "aeolianite" beds (Text-fig. 2), which indicate not only a changeable climate at the beginning of the marine Fatra Formation transgression, but also show the petrographic character of the emerged Vindelician Land yielding fine clastic material brought into the marine basin as it formed.

## SAMPLE MATERIAL AND METHODS

The Kardolína section belongs to the Bujačí partial nappe (a part of the Krížna Nappe) and it is situated on a steep western slope (the Husár Hill) of Mt Lendacká Pálenica (NNE of the village of Tatranská Kotlina) in the Belianske Tatry Mts (GPS coordinates: N49°14′997″ and E20°18′894″; Text-fig. 1). In this well-exposed, 122-m-thick section, we concentrated on its lower part (the "aeolianite cycle", Beds 12 to 14) (Text-fig. 2), where 15 sedimentary rock samples were taken and macroscopically described.

From all samples, polished thin sections were prepared for microscopic study. To document the mineral composition and microscopic texture of the different studied rock types, polarising microscopy was carried out using a ZEISS AXIO Scope.A1. Photomicrographs were obtained with a digital camera (Axiocam 105 color) coupled with AxioVision SE64 Rel. 4.9.1 Software.

The CL microscopy was performed on nine carbon-coated thin sections using a hot-cathode luminescence microscope (*lumic Simon-Neuser* HC5-LM) at the Department of Lithospheric Research, Faculty of Earth Sciences, Geography and Astronomy, University of Vienna. This microscope allowed the observation of a relatively large area of the same sample in luminescent, plane-polarised, and cross-polarised light. The system was operated with a beam energy of 14 kV and a beam current of 0.25–0.30 mA at a vacuum of 1.0E-5 mbar. Luminescence images were captured during CL operations by means of a digital high-sensitivity camera (CCD Kappa PS 4/40) equipped with the Kappa Camera Control: DX40C-285GE software package. The exposure time for recording CL images was about 1–4 s. CL spectra were not recorded, because no spectrograph was attached to the CL microscope. Therefore, CL colours were established visually. Interpretation of luminescence mineralogical observations was complemented by comparison with plane-polarised and cross-polarised transparencies of the same field of view.

## GENERAL PETROGRAPHY OF THE STUDIED ROCKS

Three main rock groups were identified within the samples studied: dark grey fine detrital argillaceous limestones (Text-fig. 3a, b), dark brown aleuritic marlstones (Text-fig. 3c, d), and dark grey carbonate mudstones (Text-fig. 3e, f).

The dominant component of the argillaceous limestones is carbonate mud. In this extremely fine-grained carbonate mud, various shell fragments of different sizes are embedded (Text-fig. 3a, b). Two principal types of fragments are present. At first, there are fragments with a regular, layered structure. These are shells which have been preserved in their original calcite composition. Further, there are pieces of originally aragonite shells, in which the metastable aragonite has just been replaced by calcite sparite. The pelitic matrix of the argillaceous limestones contains a sporadic silty admixture consisting of angular quartz grains (0.04 to 0.1 mm).

The aleuritic marlstones or marly siltstones are made up of angular fine fragments of clastic material (mainly quartz, rarely mica flakes) and a clay matrix with an abundant carbonate admixture (Text-fig. 3c, d). Frequent angular quartz grains attaining diam-

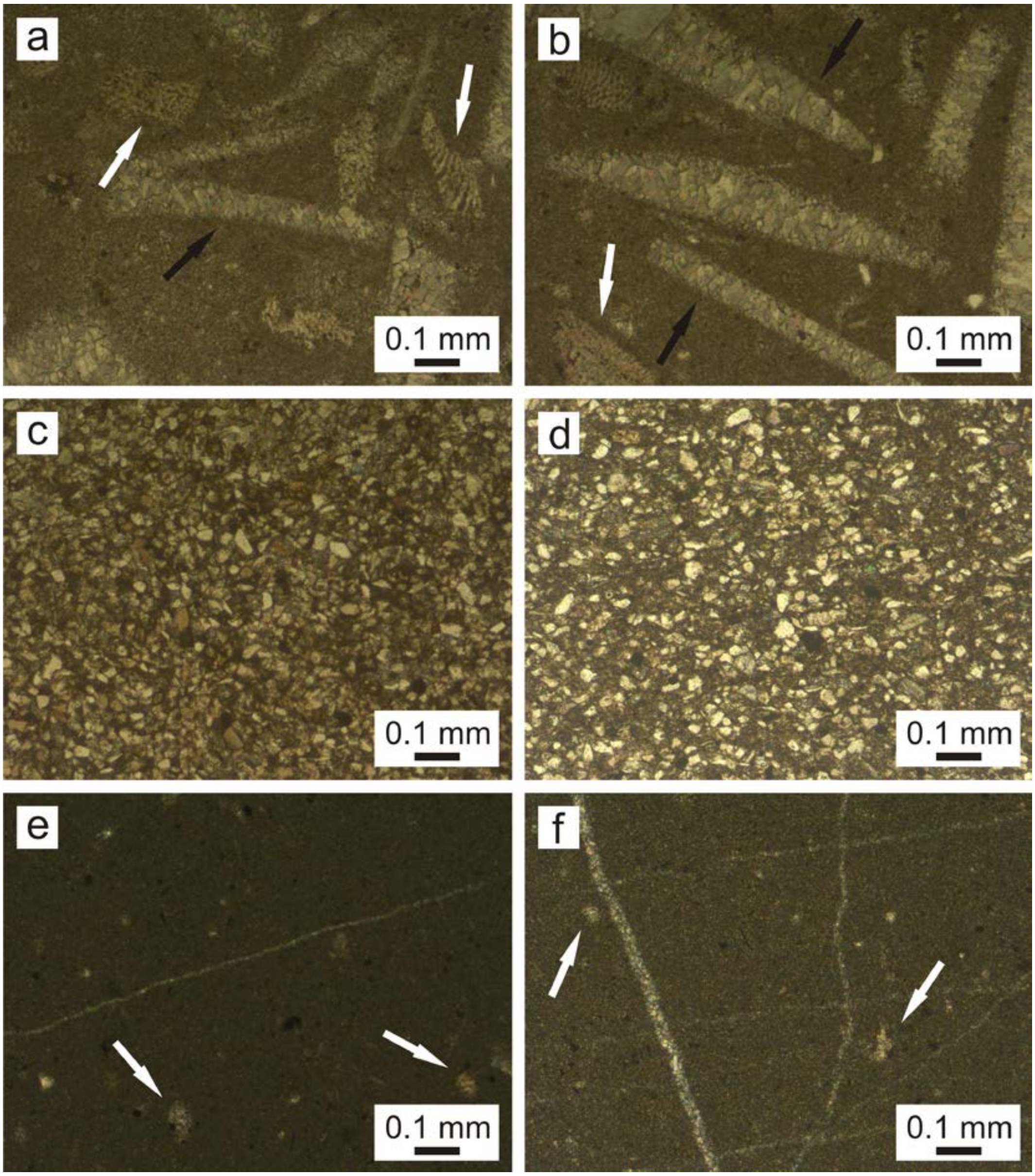


Text-fig. 3. Selected thin-section photomicrographs of the studied sedimentary rocks showing characteristic fabrics and component distributions. a, b – argillaceous limestones with micritic matrix (calcimudstones); crinoids (white arrows) and bivalves (black arrows) are present; c, d – aleuritic marlstones/marly siltstones containing windblown silt-sized quartz grains; e, f – carbonate mudstones with micritic matrix (calcimudstones) crossed by sparry calcite-filled veins; rare small bioclasts (white arrows) can be seen. All pictures are taken in transmitted light, with parallel nicols.

eters of 0.02 to 0.08 mm suggest aeolian transport. Aeolian deposition is indicated by the narrow size range of the grains, good overall sorting, winnowing out of fine particles, and angular to subangular shapes of all quartz grains. In these rocks, the stratification is characterised by different grain size, colour, and composition of the laminae. Calcite shell fragments were observed very rarely.

Finally, with a few indistinct bioclasts visible, the carbonate mudstones studied are almost completely made of carbonate mud (Text-fig. 3e, f). In general, these rocks contain less than 10% allochems. Furthermore, they are cut by thin veins of pale calcite. According to Folk's classification (Folk 1959, 1962), our carbonate mudstones represent fossiliferous micrite.

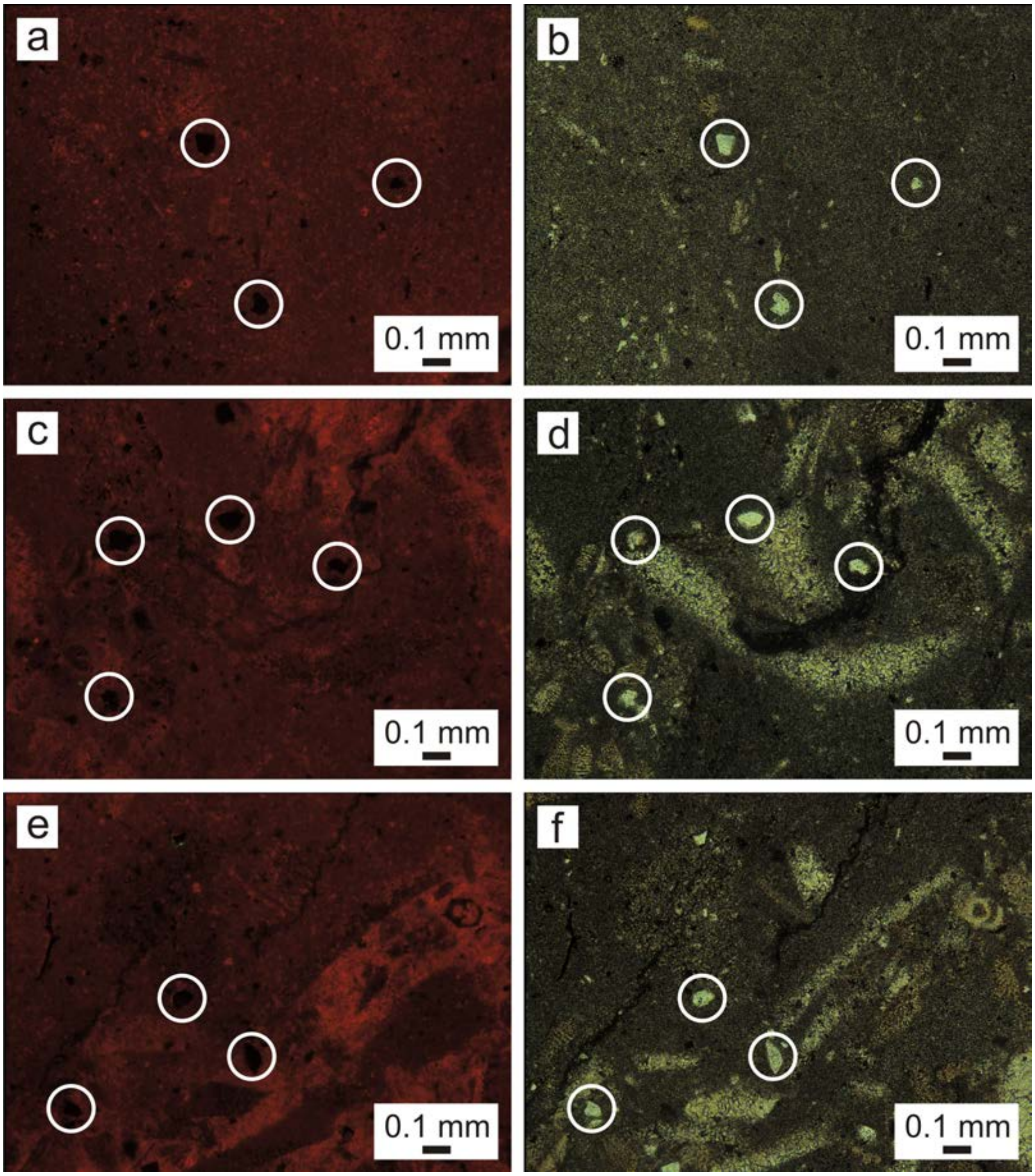


Text-fig. 4. Luminescence (a, c, and e) one polariser (b, d, and f) pairs of the studied argillaceous limestones with very dark blue or grey to bluish black quartz grains (circled in white). For explanation of provenance significance of the observed CL colours, see Cathodoluminescence Colours of Quartz Grains.

## CATHODOLUMINESCENCE COLOURS OF QUARTZ GRAINS

Samples with lower carbonate contents (mainly aleuritic marlstones/marly siltstones) and CL colours in quartz unaffected by post-depositional processes (differential compaction, solution, and cementation) were chosen for the CL study. In this study, the distribution of randomly found quartz grains with diverse CL colours was used as a guide for their source rocks.

Generally, the CL study reveals very dark blue (grey) to bluish black, green, brown, and bright and medium blue to violet luminescence of quartz grains (Text-figs 4, 5, 6). All these quartz types are presented and discussed next.

Most of the quartz particles (more than 90%) show very dark blue or grey to bluish black CL colours (Text-figs 4, 5, 6). In fact, these particles do not appear to be luminescent. Presumably, the loss of the luminescence may reflect cleaning of the quartz lattices from trace elements and defects (see also Ramseyer 1983). Non-luminescent quartz

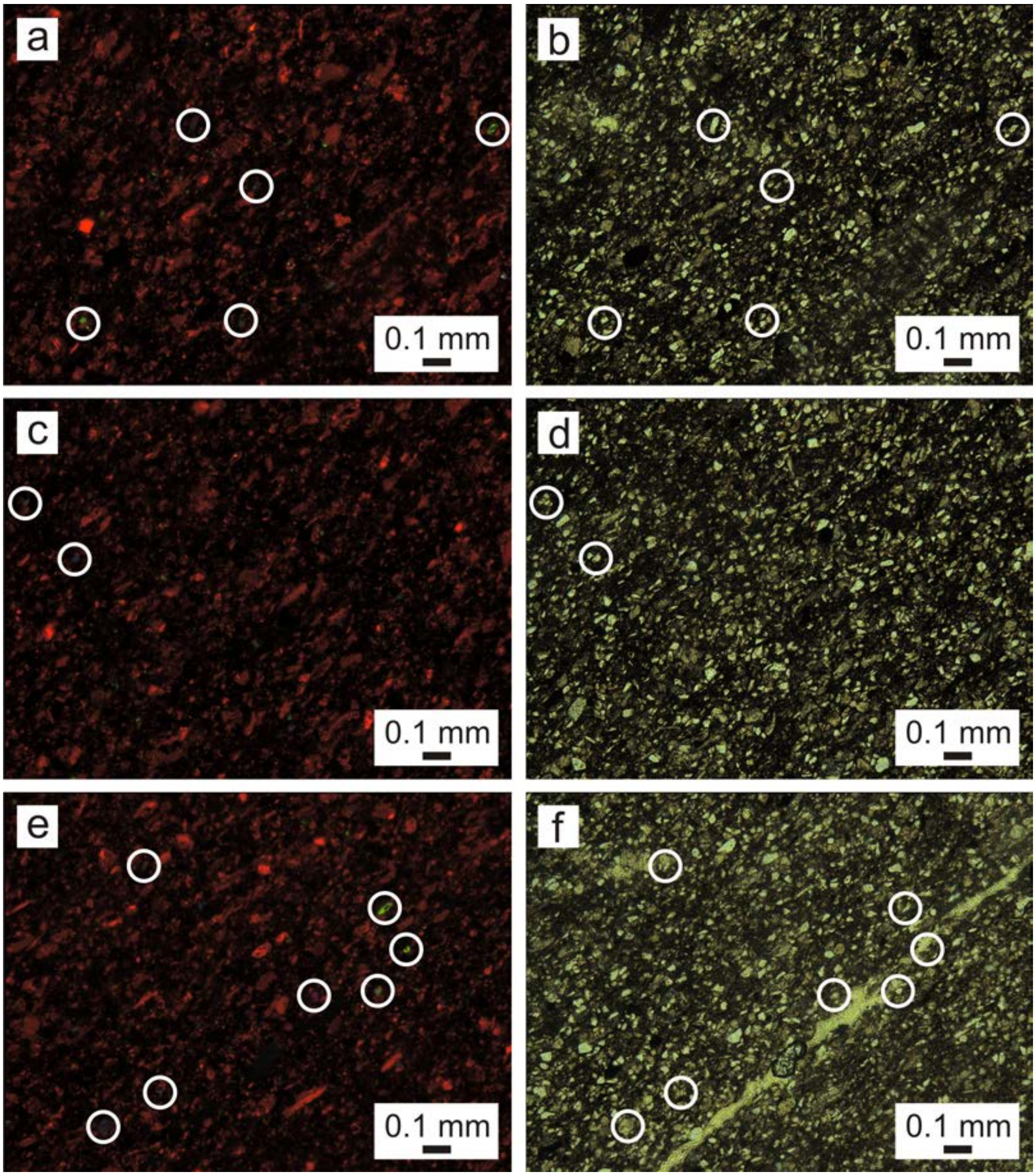


Text-fig. 5. Luminescence (a, c, and e) one polariser (b, d, and f) pairs of the studied aleuritic marlstones/marly siltstones. Very dark blue (grey) to bluish black quartz grains are dominant. However, some quartz grains (circled in white) display green, brown, and bright and medium blue to violet CL colours. Quartz grains with cement rims can also be noticed. For explanation of provenance significance of the observed CL colours, see Cathodoluminescence Colours of Quartz Grains.

grains have an authigenic origin (e.g. Zinkernagel 1978; Ramseyer *et al.* 1988; Götze 1996; Boggs 2009). However, the petrographic features of these studied quartz grains (their overall morphology) clearly exclude that they are diagenetically grown. Matter and Ramseyer (1985) observed bluish black luminescence in plutonic quartz crystals which have been plastically deformed. According to these authors, the change from the original blue to this dull colour represents the effect of a reduced intensity of luminescence. Further, and this is also our case, this type is most abundant in geologically old sedimentary rocks. According to the atlas of Sawatzky and Pe-Piper (2012), quartz grains displaying very dark blue or grey luminescence are derived from quartz veins of metapelites, low-grade metamorphic rocks (quartzites), or high-pressure metamorphic rocks (foliated metasandstones). Therefore, we suppose that the studied quartz grains of this first type could have originated in these source rocks.

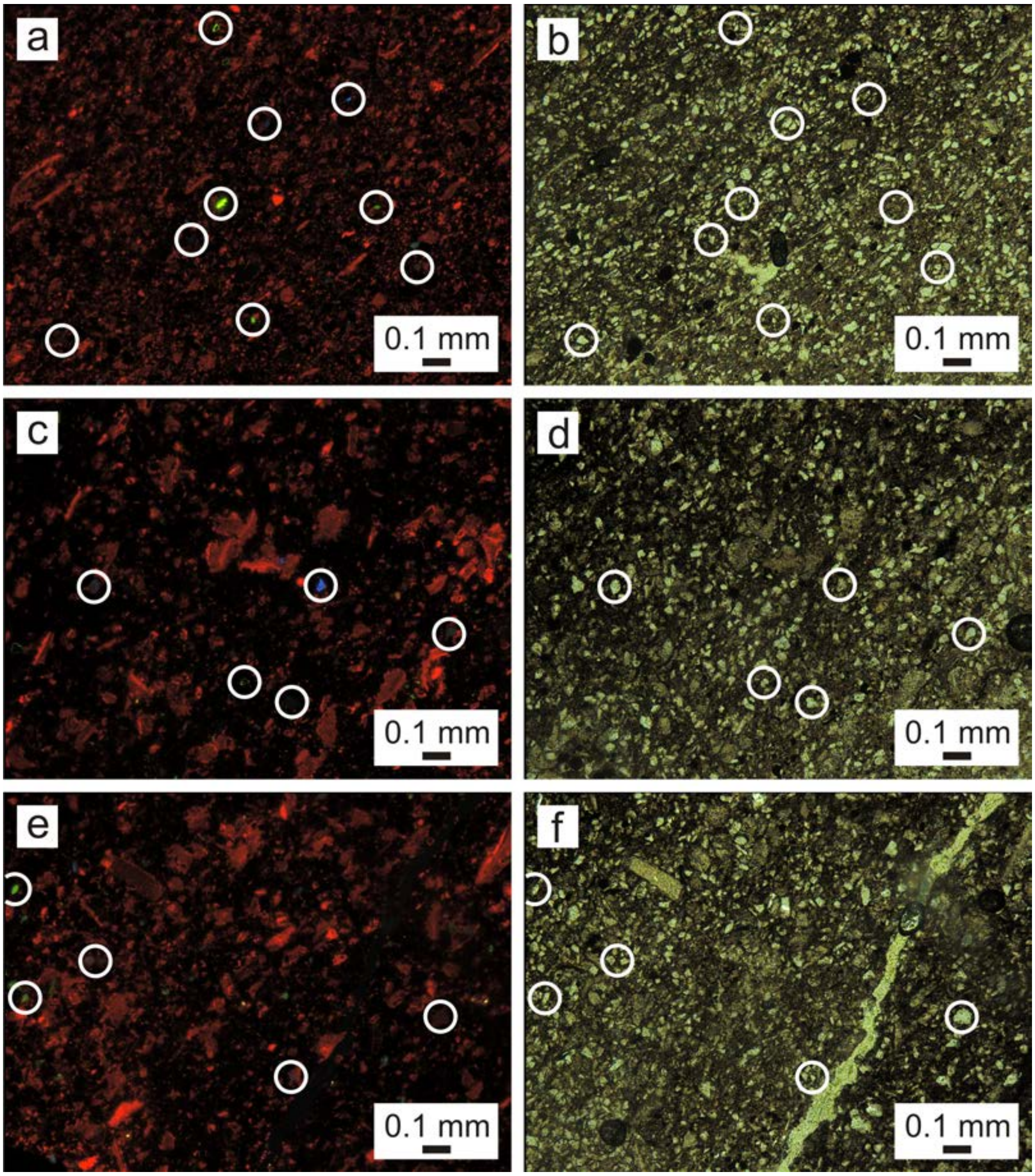


Text-fig. 6. Luminescence (a, c, and e) one polariser (b, d, and f) pairs of the studied aleuritic marlstones/marly siltstones. There is a dominance of very dark blue (grey) to bluish black quartz grains. A few quartz grains (circled in white) are green, brown, and bright and medium blue to violet. Quartz grains with cement rims are also present. For explanation of provenance significance of the observed CL colours, see Cathodoluminescence Colours of Quartz Grains.

A part of the quartz grains (about 5%) show a typical green CL colour (Text-figs 5a, e, 6a, e). This short-lived green luminescence colour clearly indicates a relationship with the crystal structure of these quartz grains and is probably stimulated by positively charged trace elements ($H^+$ or $Li^+$) stored in structural channels parallel to the c-axis of the crystals (see also Matter and Ramseyer 1985). For example, Götze *et al.* (2001) suggest that the short-lived bottle-green or blue CL in $\alpha$-quartz is another conspicuous feature of quartz CL and is typical of quartz crystallised from hydrothermal solutions. In addition, Götte and Richter (2006) report that the CL properties of hydrothermal quartz are highly variable and may reflect disequilibrium conditions during crystal growth. Nevertheless, many authors demonstrate that short-lived green luminescing quartz grains are of hydrothermal and pegmatite origin (e.g. Götze and Zimmerle 2000; Boggs and Krinsley 2006; Augustsson and Reker 2012; Sawatzky and Pe-Piper 2013). Thus, we also assume such an origin for this second group of the studied quartz grains.

Several quartz grains (about 2%) display brown luminescence (Text-figs 5a, e, 6). This brown CL colour can be related to lattice defects induced by twinning, mechanical deformation, particle bombardment, or rapid growth (see also Ramseyer *et al.* 1988; Götze *et al.* 2001). Zinkernagel (1978) reported that quartz grains with brown luminescence are derived from metasediments, metamorphosed igneous rocks, some contact metamorphic rocks, and regionally metamorphosed rocks. Subsequently, many workers concluded that brown luminescent quartz is typical of regionally low to medium grade metamorphosed rocks (e.g. Matter and Ramseyer 1985; Götze 1996; Boggs and Krinsley 2006; Sales de Oliveira *et al.* 2017). These rocks could represent the potential sources for this group of the studied quartz grains.

A few quartz grains (about 2%) show bright and medium blue to violet CL colours (Text-figs 5, 6). These luminescence colours are probably caused by different kinds of lattice defects (see also Matter and Ramseyer 1985) and/or high amounts of titanium and low iron contents (see also Sprunt 1981). According to Augustsson and Bahlburg (2003), bright blue luminescence of quartz is generated by crystallisation at high temperatures and fast cooling. These quartzes usually appear in volcanic rocks or rocks affected by contact metamorphism. Also, with lower crystallisation temperatures and slower cooling, the cathodoluminescence signal of quartz is less intense, and the particles usually appear dark blue. This type is frequent in plutonic rocks, due to their slower cooling rates than those of volcanics (Augustsson and Bahlburg 2003). Moreover, it is generally assumed that a wide variation of luminescence colours from blue through mauve to violet is typical of felsic plutonic quartz, quartz phenocrysts in volcanic rocks, and high-grade metamorphic quartz (e.g. Boggs and Krinsley 2006; Boggs 2009; Augustsson and Reker 2012; Sawatzky and Pe-Piper 2013). Thus, our blue to violet luminescing quartz grains could be derived from plutonic igneous, volcanic, and high-grade metamorphic rocks. However, the contribution from volcanic rocks can be excluded because our studied blue to violet quartz grains display dark-CL streaks and patches, which is the most characteristic feature of plutonic quartz crystals (see also Boggs 2009).

In addition to the above, some of the quartz grains (about 1%) have relict cement rims (Text-figs 5a, e, 6a, c). These recycled quartz cement overgrowths probably indicate reworking of older sedimentary rocks and thus an at least second cycle origin (see also Götte and Richter 2006). However, it is difficult to prove which grains are of primary and which of secondary origin because of the quartz size. Quartz grains are so small here that they all may represent just fragments of larger secondary as well as primary pieces.

Finally, no red luminescing quartz grains have been observed during the CL study. Therefore, we do not assume derivation from any volcanic rocks.

## PROVENANCE STUDY

The CL study shows a dominance of quartz particles of regional metamorphic and plutonic origin. Also, this study reveals that the sedimentary rock samples contain a smaller population of quartz grains with possible hydrothermal and pegmatite origins. Presumably, this higher variability of quartz grains reflects a large catchment area providing material for

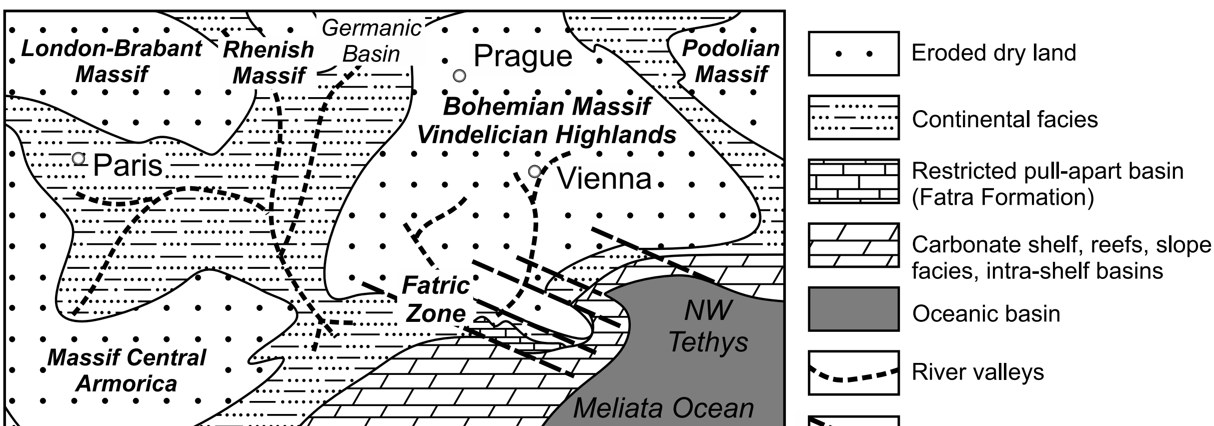


Text-fig. 7. Palaeogeographic map of the Late Triassic showing the approximate location of the sedimentary site of the Fatra Formation (modified from Lintnerová *et al.* 2013; Onoue *et al.* 2022).

the depositional basin. This area could be also small but diverse in rock types. Quartz grains with cement rims indicate that they are at least second-cycle and they probably contribute to the higher variability in the source rocks. In addition, the CL study shows that red luminescent quartz particles with a potential volcanic origin are absent.

Because we did not record any population of particles from volcanic sources, we exclude deposition in, or close to, a convergent plate tectonic margin associated with volcanism. The dominance of quartz particles that obtained their CL characteristics during metamorphic or plutonic conditions can be expected from active tectonic margins with no volcanism or from passive margins. Sedimentary rocks deposited along passive continental margins can be expected to be dominated by quartz particles of metamorphic, plutonic, and recycled affinities. Consequently, the sedimentary rocks studied were probably deposited in a passive margin environment and fed by sources from the old continental interior.

The above mentioned findings coming from the CL study are in accordance with the palaeogeographic model used by Michalík (1994), Feist-Burkhardt *et al.* (2008), Lintnerová *et al.* (2013), Čerňanský *et al.* (2020), and Onoue *et al.* (2022). Thus, we also assume that the studied quartz grains could have originated in the rocks of the Vindelician Highlands (Text-fig. 7). Products of volcanic activity from the Mid-Atlantic Rift have not been recorded. It might also be added that the arid interior along the northern Tethyan coast rimmed by the Vindelician Range has been formed in rain shadow, being isolated from summer monsoonal rains. On the other hand, winter winds brought fine dust from desert plains of the Germanic Basin across the highlands towards the south-east.

## CONCLUSIONS

The studied "aeolianite" beds at the base of the Fatra Formation (Western Carpathians, Slovakia) indicate both a changeable dry climate at the beginning of the marine Fatra Formation transgression and the petrographic character of the emerged Vindelician Land, which represented the source area of fine clastic quartz grains brought, as it formed, into the marine Zliechov Basin. By using CL microscopy, the sedimentary rocks studied show several different quartz types reflecting a variable provenance with regional metamorphic, plutonic, hydrothermal, pegmatite, and sedimentary source rocks. Products of volcanic activity from the Mid-Atlantic Rift can be excluded. Thus, in respect of their tectonic setting, the sedimentary rocks were deposited in a passive margin environment.

## Acknowledgements

We thank P. Jaglarz and an anonymous reviewer for their considered comments and suggestions, which helped to strengthen the paper. Editor-in-Chief P. Łuczyński is thanked for careful management of the manuscript. Furthermore, the authors wish to thank D. Mader (University of Vienna) for his support during laboratory measurements and Š. Pramuková (Earth Science Institute of the Slovak Academy of Sciences) for the preparation of thin sections. Field work could not have been done without the help of Z. Zrubáková. This research was financially supported by the Scientific Grant Agency of the Ministry of Education, science, research and sport of the Slovak Republic and the Slovak Academy of Sciences under grant VEGA 2/0090/19.

## REFERENCES

Augustsson, C. and Bahlburg, H. 2003. Cathodoluminescence spectra of detrital quartz as provenance indicators for Paleozoic metasediments in southern Andean Patagonia. *Journal of South American Earth Sciences*, **16**, 15–26.

Augustsson, C. and Reker, A. 2012. Cathodolumenescence spectra of quartz as provenance indicators revisited. *Journal of Sedimentary Research*, **82**, 559–570.

Boggs, S. Jr. 2009. Petrology of sedimentary rocks, 600 pp. Cambridge University Press; New York.

Boggs, S. Jr. and Krinsley, D. 2006. Application of cathodoluminescence imaging to the study of sedimentary rocks, 165 pp. Cambridge University Press; New York.

Čerňanský, A., Klein, N., Renesto, S., Michalík, J., Šurka, J. and Sentpetery, M. 2020. The first skeletal evidence of an Upper Triassic (Rhaetian) diapsid reptile from the Western Carpathians (Strážov Highlands, Slovakia). *Geologica Carpathica*, **71**, 134–149.

Feist-Burkhardt, S., Götz, A.E., Szulc, J., Borkhataria, R., Geluk, M., Haas, J., Hornung, J., Jordan, P., Kempf, O., Michalík, J., Nawrocki, J., Reinhardt, L., Ricken, W., Röhling, H.-G., Rüffer, T., Török, Á. and Zühlke, R. 2008. Triassic. In: McCann, T. (Ed.), The Geology of Central Europe. Volume 2: Mesozoic and Cenozoic, 749–821. Geological Society; London.

Folk, R.L. 1959. Practical petrographic classification of limestones. *AAPG Bulletin*, **43**, 1–38.

Folk, R.L. 1962. Spectral subdivision of limestone types. In: Ham, W.E. (Ed.), Classification of carbonate rocks – a symposium, 62–84. The American Association of Petroleum Geologists; Tulsa.

Gaździcki, A. 1983. Foraminifers and biostratigraphy of Upper Triassic and Lower Jurassic of the Slovakian and Polish Carpathians. *Palaeontologia Polonica*, **44**, 109–169.

Gaździcki, A., Michalík, J., Planderová, E. and Sýkora, M. 1979. An Upper Triassic–Lower Jurassic sequence in the Krížna nappe (West Tatra mountains, West Carpathians, Czechoslovakia). *Západné Karpaty, séria geológia*, **5**, 119–148.

Götte, Th. and Richter, D.K. 2006. Cathodoluminescence characterization of quartz particles in mature arenites. *Sedimentology*, **53**, 1347–1359.

Götze, J. 1996. Kathodolumineszenz von Quarz – Grundlagen und Anwendung in den Geowissenschaften. *Aufschluss*, **47**, 145–164.

Götze, J., Plötze, M. and Habermann, D. 2001. Origin, spectral characteristics and practical applications of the cathodoluminescence (CL) of quartz – a review. *Mineralogy and Petrology*, **71**, 225–250.

Götze, J. and Zimmerle, W. 2000. Quartz and silica as guide to provenance in sediments and sedimentary rocks. *Contributions to Sedimentary Geology*, **21**, 1–91.

Leila, M., Moscariello, A. and Šegvić, B. 2018. Geochemical constraints on the provenance and depositional environment of the Messinian sediments, onshore Nile Delta, Egypt: Implications for the late Miocene paleogeography of the Mediterranean. *Journal of African Earth Sciences*, **143**, 215–241.

Lintnerová, O., Michalík, J., Uhlík, P., Soták, J. and Weissová, Z. 2013. Latest Triassic climate humidification and kaolinite formation (Western Carpathians, Tatric Unit of the Tatra Mts.). *Geological Quarterly*, **57**, 701–728.

Marshall, D.J. 1988. Cathodoluminescence of geological materials, 138 pp. Unwin Hyman; London.

Matter, A. and Ramseyer, K. 1985. Cathodoluminescence microscopy as a tool for provenance studies of sandstones. In: Zuffa, G.G. (Ed.), Provenance of arenites, 191–211. D. Reidel Publishing Company; Dordrecht.

Michalík, J. 1974. Zur Paläogeographie der rätischen Stufe des westlichen Teils der Krížna-Decke in den Westkarpaten. *Geologický Zborník – Geologica Carpathica*, **25**, 257–285.

Michalík, J. 1977. Paläogeographische Untersuchungen der Fatra-Schichten (Kössen-Formation) des nördlichen Teiles des Fatrikums in den Westkarpaten. *Geologický Zborník – Geologica Carpathica*, **28**, 71–94.

Michalík, J. 1982. Uppermost Triassic short-lived bioherm complexes in the fatric, western Carpathians. *Facies*, **6**, 129–145.

Michalík, J. 1993. Mesozoic tensional basins in the Alpine-Carpathian shelf. *Acta Geologica Hungarica*, **36**, 395–403.

Michalík, J. 1994. Notes on the paleogeography and paleotectonics of the Western Carpathian area during the Mesozoic. *Mitteilungen der Österreichischen Geologischen Gesellschaft*, **86**, 101–110.

Michalík, J., Biroň, A., Lintnerová, O., Götz, A.E. and Ruckwied, K. 2010. Climate change at the Triassic/Jurassic boundary in the northwestern Tethyan realm, inferred from sections in the Tatra Mountains (Slovakia). *Acta Geologica Polonica*, **60**, 535–548.

Michalík, J., Kátlovský, V. and Hluštík, A. 1988. Plant remains in the Tomanová Formation (Uppermost Triassic, West Carpathians): their origin, composition and diagenetic alteration. *Geologický Zborník – Geologica Carpathica*, **39**, 523–537.

Michalík, J., Lintnerová, O., Gaździcki, A. and Soták, J. 2007. Record of environmental changes in the Triassic–Jurassic boundary interval in the Zliechov Basin, Western Carpathians. *Palaeogeography, Palaeoclimatology, Palaeoecology*, **244**, 71–88.

Michalík, J., Lintnerová, O., Wójcik-Tabol, P., Gaździcki, A., Grabowski, J., Golej, M., Šimo, V. and Zahradníková, B. 2013. Paleoenvironments during the Rhaetian transgression and the colonization history of marine biota in the Fatric Unit (Western Carpathians). *Geologica Carpathica*, **64**, 39–62.

Michalík, J., Planderová, E. and Sýkora, M. 1976. To the stratigraphic and paleogeographic position of the Tomanová-formation in the uppermost Triassic of the West Carpathians. *Geologický Zborník – Geologica Carpathica*, **27**, 299–318.

Niedźwiedzki, G. 2005. A new find of dinosaur footprints in the Upper Triassic of the Tatra Mountains, southern Poland. *Przegląd Geologiczny*, **53**, 410–413.

Niedźwiedzki, G. 2011. A Late Triassic dinosaur-dominated ichnofauna from the Tomanová Formation of the Tatra Mountains, Central Europe. *Acta Palaeontologica Polonica*, **56**, 291–300.

Omer, M.F. 2015. Cathodoluminescence petrography for provenance studies of the sandstones of Ora Formation (Devonian–Carboniferous), Iraqi Kurdistan Region, northern Iraq. *Journal of African Earth Sciences*, **109**, 195–210.

Onoue, T., Michalík, J., Shirozu, H., Yamashita, M., Yamashita, K., Kusaka, S. and Soda, K. 2022. Extreme continental weathering in the northwestern Tethys during the end-Triassic mass extinction. *Palaeogeography, Palaeoclimatology, Palaeoecology*, **594**, 110934.

Ramseyer, K. 1983. Bau eines Kathodenlumineszenz-Mikroskopes und Diagenese-Untersuchungen an permischen Sedimenten aus Oman. Unpublished PhD Thesis, 152 pp. University of Bern; Bern.

Ramseyer, K., Baumann, J., Matter, A. and Mullis, J. 1988. Cathodoluminescence colours of α-quartz. *Mineralogical Magazine*, **52**, 669–677.

Sales de Oliveira, C.E., Pe-Piper, G., Piper, D.J.W., Zhang, Y. and Corney, R. 2017. Integrated methodology for determining provenance of detrital quartz using optical petrographic microscopy and cathodoluminescence (CL) properties. *Marine and Petroleum Geology*, **88**, 41–53.

Sawatzky, C. and Pe-Piper, G. 2012. Provenance identification of detrital quartz using hot-cathode cathodoluminescence: An atlas of source rocks, 149 pp. Geological Survey of Canada; Halifax.

Sawatzky, C.C. and Pe-Piper, G. 2013. Detrital quartz sources in the Scotian Basin, eastern Canada, using hot-cathode cathodoluminescence: Availability of coarse-grained sand for reservoirs. *AAPG Bulletin*, **97**, 1503–1520.

Sippel, R.F. 1968. Sandstone petrology, evidence from luminescence petrography. *Journal of Sedimentary Petrology*, **38**, 530–554.

Sprunt, E.S. 1981. Causes of quartz cathodoluminescence colors. *Scanning Electron Microscopy*, **1**, 525–535.

Tomašových, A. 2004. Microfacies and depositional environment of an Upper Triassic intra-platform carbonate basin: the Fatric Unit of the West Carpathians (Slovakia). *Facies*, **50**, 77–105.

Tomašových, A. and Michalík, J. 2000. Rhaetian/Hettangian passage beds in the carbonate development in the Krížna Nappe (central Western Carpathians, Slovakia). *Slovak Geological Magazine*, **6**, 241–249.

Zinkernagel, U. 1978. Cathodoluminescence of quartz and its application to sandstone petrology. *Contributions to Sedimentology*, **8**, 1–69.

*Manuscript submitted: 11th July 2022*
*Revised version accepted: 2nd December 2022*